Environmental Science & Technology

Article

Cite This: Environ. Sci. Technol. 2019, 53, 8352−8361

pubs.acs.org/est

Electro-Forward Osmosis

Moon Son,[†] Taeyoung Kim,[‡] Wulin Yang,[†] Christopher A. Gorski,[†] and Bruce E. Logan*[,†]

[†]Department of Civil and Environmental Engineering, The Pennsylvania State University, University Park, Pennsylvania 16802, United States

[‡]Department of Chemical and Biomolecular Engineering, and Institute for a Sustainable Environment, Clarkson University, Potsdam, New York 13699, United States

Supporting Information

ABSTRACT: The impact of ion migration induced by an electrical field on water flux in a forward osmosis (FO) process was examined using a thin-film composite (TFC) membrane, held between two cation exchange membranes. An applied fixed current of 100 mA (1.7 mA cm^{-2}) was sustained by the proton flux through the TFC-BW membrane using a feed of 34 mM NaCl, and a 257 mM NaCl draw solution. Protons generated at the anode were transported through the cation exchange membrane and into the draw solution, lowering the pH of the draw solution. Additional proton transport through the TFC-BW membrane also lowered the pH of the feed solution. The localized accumulation of the protons on the draw side of the TFC-BW membrane resulted in high concentration polarization modulus of 1.41 × 10^5, which enhanced the water flux into the draw solution (5.56 LMH at 100 mA), compared to the control (1.10 LMH with no current). These results using this electro-forward osmosis (EFO) process demonstrated that enhanced water flux into the draw solution could be achieved using ion accumulation induced by an electrical field. The EFO system could be used for FO applications where a limited use of draw solute is necessary.

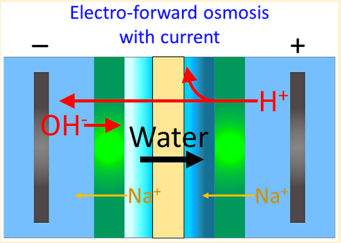

INTRODUCTION

In recent decades, osmosis-driven processes such as forward osmosis (FO) have been extensively investigated in separation processes for wastewater treatment, food processing, and seawater/brackish water desalination due to its reduced susceptibility to fouling and low energy consumption compared to pressure-driven processes.[1,2] To improve the utility of the osmosis-driven processes, it is desirable to increase water flux. One approach is pressure-assisted FO (PAO),[3−6] which uses additional pressure to force water through the membrane. However, potential membrane deformation has limited the utility of this approach.[3,4] An alternative method was developed in the field of electrochemistry based on applying an electrical field, using an over limiting current (OLC), to create a concentration gradient of saline water across a porous frit.[7,8] However, it is not clear how successfully this process could be scaled up due to the need to pump water through a thin glass frit. Thus, other approaches are needed in order to improve water flux.

Concentration polarization (CP) of the solute, on the surface or inside of the membrane, often limits the water flux in FO and pressure-driven processes, such as reverse osmosis (RO). Several approaches have therefore been developed to minimize the impact of CP on water flux, such as depositing a hydrophilic substance on the membrane or fabricating double-skinned membranes to minimize CP inside the membrane.[9−12] However, these approaches have not been successful in significantly increasing water fluxes. An alternative method, electrolysis-assisted FO has been examined to disrupt ion movement by using an electric field, but it has only been successful in mitigating reverse solute flux, not increasing water flux.[13] In addition, there have been studies demonstrating that that fouling was reduced by applying a voltage across the feed solution,[14] or water permeation was controlled through a thin electrically conductive membrane such as graphene,[15] but there are no previous studies showing an increased water flux across a thin-film membrane with an applied electrical current.

Here, we demonstrate that water flux into the draw solution can be enhanced by developing a localized high concentration of protons on the draw side of the thin-film composite membrane through current generation and water splitting at the anode (which releases protons into solution). This system, called an electro-forward osmosis system (EFO), was constructed by creating two chambers on either side of a composite thin-film membrane, enclosed by two cation exchange membranes. The electrolyte chambers were on the other sides of the cation exchange membranes, and a model salt of sodium chloride solution was used. By applying a set current to produce protons at the anode, a CP layer could be developed on the draw side of the membrane, resulting in an enhanced water flux. The functioning of this system was examined using two different thin-film composite membranes, in the presence and absence of cation exchange membranes or with different ion exchange membranes, and by changing the salt concentrations and pH values of the sodium chloride solutions. The impact of the chloride ion in the water was further examined using sodium nitrate as the salt.

Received: March 9, 2019
Revised: June 2, 2019
Accepted: June 18, 2019
Published: June 18, 2019

DOI: 10.1021/acs.est.9b01481
Environ. Sci. Technol. 2019, 53, 8352−8361

MATERIALS AND METHODS

EFO Cell Construction with Two Ion Exchange Membranes. All experiments were performed using a commercial electrodialysis cell (PCCell 64002) and titanium electrodes with a coating of platinum/iridium. The electrodialysis cell contained four channels separated by two ion exchange membranes, and a polymer membrane in the middle (Figure 1 and Supporting Information (SI) Figure S1). The

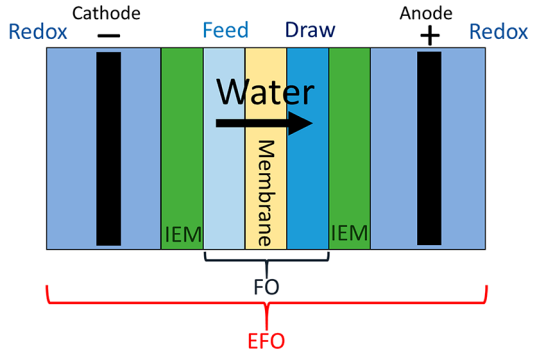

Figure 1. Schematic of the electro-forward osmosis (EFO) system. In the forward osmosis (FO) compartment, a thin-film composite membrane was used as a FO membrane. Different concentrations of salt solution, 34 mM (feed), 145 mM (redox), and 257 mM (draw), were used to test the water flux of the system. The redox chambers having electrodes (black bars) were used to provide the set current across the system, and ion exchange membranes, IEMs (either cation or anion exchange membranes), were placed between the FO compartment and redox chambers for the stability of the EFO system. Overall charge balance across the system is maintained mostly by proton movement. Protons generated at the anode migrated to the draw solution and accumulated on the membrane surface resulting in water flux enhancement from the feed to draw solution due to increased osmotic pressure generated by protons.

ion exchange membranes were cation exchange membranes (CEMs), except as indicated when one of these membranes was switched to an anion exchange membrane (AEM). Woven spacers inserted between membranes and chambers were 375 ± 4 μm thick, and had a width and length of 7.7 cm, producing an effective membrane area of 59 cm^2. The length, width, and depth of the redox chambers were ~7.7 × 7.7 × 0.4 cm^3. Flow rates for the feed (5 mL min^{-1}), draw (5 mL min^{-1}), and redox (30 mL min^{-1}) solutions were controlled by peristaltic pumps (Masterflex) using silicone tubing 1.6 mm (inner diameter). The flow rates for each chamber were selected based on preliminary tests of 5−30 mL min^{-1} and achieving stable voltage changes for different set current (100−300 mA). The lowest flow rate was chosen to minimize energy input into the system. Current was set at ~0.4 mA cm^{-2} (25 mA) or ~1.7 mA cm^{-2} (100 mA) using a potentiostat (VMP3, Bio-Logic), and the resulting voltage was recorded during operation.

Ion Exchange and Polymer Membranes. The polymer membranes were either a polyamide based thin-film composite (TFC) membranes designated for seawater (TFC-SW), or brackish water (TFC-BW) desalination, purchased from Dow Filmtech. The TFC-SW (SW30HR) membrane had a thickness of 130 ± 4 μm and TFC-BW (BW30LE) had a thickness of 123 ± 5 μm. The pore size of a cross-linked polyamide layer of TFC membranes is generally given as ~0.25 nm, even though the TFC-BW membrane is known to have a higher permeability than the TFC-SW membrane due to less polyamide cross-linking.[16,17] One of the main attributes of the TFC-BW membrane is that it has a more positive surface charge at lower pH values than the TFC-SW membrane.[18,19] To demonstrate the concept of EFO, commercial RO membranes were used here for tests due to their wide availability and relatively low cost compared to FO membranes. The CEM (Selemion CMV, Asahi Glass, Japan) had a thickness of 98 ± 1 μm and ion exchange capacity of 2.08 mmol/g. The AEM (Selemion AMV, Asahi Glass, Japan) was 106 ± 1 μm thick with an ion exchange capacity of 1.85 mmol/g.[20,21]

Measurement of Water Flux, Solution Conductivity, Voltage, and pH. Low salt concentration (34 mM, representative of a typical brackish feedwater), high salt concentration (257 mM, representative of draw solution), and moderate salt concentration (145 mM, used in redox chambers) solutions were prepared by dissolving NaCl (Macron Fine Chemicals) or $NaNO_3$ (Sigma-Aldrich, > 99%) in deionized water (Synergy, EMD Millipore). HCl (VWR, 36.5−38%, ACS grade), HNO_3 (VWR, 68−70%), or NaOH (J.T.Baker, Pellets) were used to adjust the pH, as indicated. The effluent conductivity was recorded using two flow-through conductivity meter electrodes (ET908, eDAQ, Australia) located at each cell outlet.[22] The pH was measured by a pH meter (SevenMulti, Mettler Toledo). Effluents from the feed and draw chambers were recycled and recirculated to separate bottles (~500 mL).

The water flux, J_w (LMH; L m^{-2} h^{-1}), was calculated as

$$J_w = \frac{\Delta V}{A_m \Delta t} \quad (1)$$

where ΔV is the volume of water decreased in the feed side (L), A_m the effective membrane area (~5.9×10^{-3} m^2), and Δt the permeation time (h). The active layer of the membrane faced the draw solution (AL-DS), except as indicated.

The reverse solute flux, J_s (molMH; mol m^{-2} h^{-1} or SMH; Siemens m^{-2} h^{-1}), was calculated as

$$J_s = \frac{\Delta(C_t V_t)}{A_m \Delta t} \quad (2)$$

where C_t and V_t are the salt concentration and the feed volume measured during operation. J_s was calculated based on changes in the solution conductivity at 1 min intervals, and expressed in units of molMH (mol m^{-2} h^{-1}), which are units widely used in FO, when there was no applied current (0 mA). SMH (Siemens m^{-2} h^{-1}) units were used when current was applied to the system (100 mA) because the solute contains both salt and other ions (H^+, OH^-).

Reactions on the Anode, Cathode, And in the Bulk Solution. The following electrode reactions are assumed for standard conditions at pH 0 (anode) or 14 (cathode) and only water:[23,24]

$$\text{anode (acidic)}: \frac{1}{2}H_2O = \frac{1}{4}O_2 + e^- + H^+$$
$$E^0 = 1.23\ \text{V vs SHE (pH 0)} \quad (3)$$

$$\text{cathode (alkaline)}: H_2O + e^- = \frac{1}{2}H_2 + OH^-$$
$$E^0 = -0.83\ \text{V vs SHE (pH 14)} \quad (4)$$

With these two reactions, protons are released at the anode along with oxygen, and hydroxide ions are produced at the

DOI: 10.1021/acs.est.9b01481
Environ. Sci. Technol. 2019, 53, 8352−8361

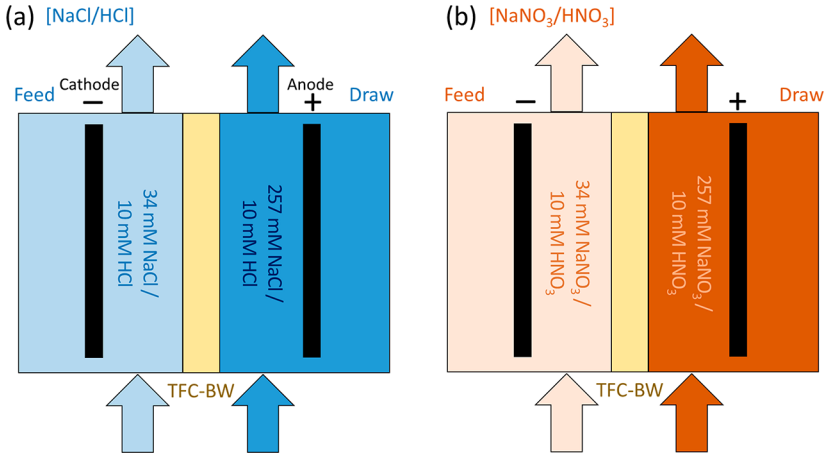

Figure 2. Schematic of the system of EFO without ion exchange membranes and redox chambers (similar to a conventional FO system, but with electrodes), showing experiments conducted using (a) NaCl/HCl or (b) $NaNO_3/HNO_3$ paired chemical species. These experiments were conducted to demonstrate the water flux with only FO (in the absence of current) or with current generation directly in the draw and feed solutions. The two different electrolytes were chosen to contrast the impact of chloride ion on the reaction at anode which competes with oxygen evolution compared to the NO_3 electrolyte which is stable and thus does not impact oxygen evolution (see eqs 3–9 for the complete reactions).

cathode. Under acidic conditions relevant to EFO operation here, however, most electrons from the cathode in the presence of only water would result in the formation of hydrogen gas, according to

$$\text{cathode (acidic): } 2H^+ + 2e^- = H_2 \quad E^0 = 0\ \text{V vs. SHE (pH 0)} \tag{5}$$

Since the solution will also contain NaCl, when a voltage is applied, chloride ions can also be oxidized to chlorine gas (Cl_2), chlorine dioxide (ClO_2), hypochlorous acid (HOCl), or hypochlorite ions (OCl^-), via the following reactions:[7,8,25−29]

$$2Cl^- = Cl_2 + 2e^- \quad E^0 = 1.45\ \text{V} \tag{6}$$

$$Cl^- + 2H_2O = ClO_2 + 4H^+ + 5e^- \quad E^0 = 1.60\ \text{V} \tag{7}$$

$$Cl_2(aq) + H_2O = HOCl + H^+ + Cl^- \quad k = 28.6\ s^{-1}\ \text{at}\ 25°C \tag{8}$$

$$HOCl = H^+ + OCl^- \quad pK_A = 7.5 \tag{9}$$

Based on the equations, there could be several products produced at the anode which could impact net production of protons, or produce chemicals that could damage the membrane. For example, if Cl_2 is produced, no protons would be released into water and instead charge is balanced by the consumption of chloride ion. All of these chloride products are oxidizers that could damage the membrane.

EFO Construction without Ion Exchange Membranes. To examine the need for the two CEMs and electrolyte chambers, additional tests were conducted using only the FO membrane (no ion exchange membranes) (Figure 2). In the absence of the CEMs, all ions produced at the electrodes are directly exposed to the feed or draw solutions. Two electrolytes were used for these tests: NaCl/HCl, and $NaNO_3/HNO_3$. By using a nitrate-based electrolyte, the possible impact of chloride-derived products could be examined as nitrate does not produce byproducts that could oxidize the membrane, and protons are released in direct proportion to the current. These tests were conducted at a constant current of 100 mA, with the nitrate electrolyte set at pH 2 to match that used with the chloride electrolyte.

Stability of the System. To assess water transport through CEMs in the EFO system, the same concentrations of NaCl solution (145 mM) were used in feed and draw sides, and DI water was used for redox chambers (SI Figure S2a).

Modeling. Membrane intrinsic parameters for water permeability (A, cm s^{-1} bar^{-1}), salt permeability (B, cm s^{-1}), and the membrane structure parameter (S, cm), were calculated using

$$A = \frac{J_w}{\Delta P} \tag{10}$$

$$B = J_w \frac{1-R}{R} \exp\left(-\frac{J_w}{k}\right) \tag{11}$$

$$R = 1 - \frac{C_p}{C_f} \tag{12}$$

where J_w is the water flux and ΔP is the applied pressure,[30,31] R is the salt rejection, k is the mass transfer coefficient,[32] C_p is the concentration of salt in the permeate solution, and C_f is the concentration of salt in the feed solution. Dead-end filtration (Sterlitech Corp., HP4750type) with a pressurized cell (N_2 gas) was used to measure water permeability and salt rejection, and concentration of salt in the solutions was measured using conductivity meter. The mass transfer coefficient of the system, k, was calculated from the Sherwood number as $Sh = kH/D$, where $H = 750\ \mu m$ is the hydraulic diameter of the channel, and $D = 1.61 \times 10^{-5}$ $cm^2 s^{-1}$ is the diffusion coefficient of the solute. The Sh was calculated from a correlation developed for systems that use the flat membranes and spacers similar to this system (see SI note).[32−34]

The membrane structure parameter (S) in FO (active layer facing feed solution) is

$$S = \left(\frac{D}{J_w}\right) \ln\left(\frac{B + A\pi_{D,b}}{B + J_w + A\pi_{F,m}}\right) \tag{13}$$

where $\pi_{D,b}$ is the osmotic pressure of bulk solution in draw side and $\pi_{F,m}$ is the osmotic pressure at the membrane surface in feed side.[32,35]

DOI: 10.1021/acs.est.9b01481
Environ. Sci. Technol. 2019, 53, 8352−8361

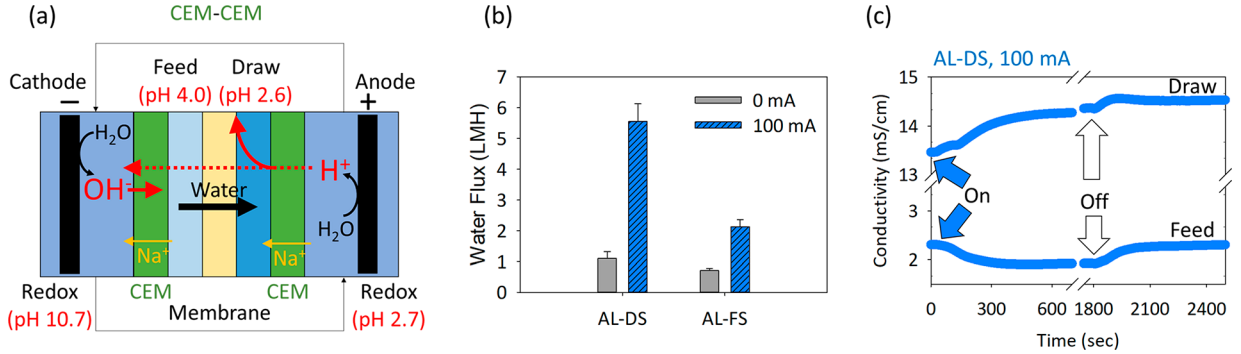

Figure 3. (a) Schematic of the EFO system with the placement of CEMs and redox chambers possessing electrodes, and the simplified movements of ions and water in the process. The pHs indicate the final conditions after operation of the system. NaCl solutions of concentrations of 34 (feed), 145 (redox), and 257 (draw) mM were used for the EFO system except as indicated. (b) Water flux of the TFC-BW membrane in the EFO system with different orientations (AL-DS, active layer faces draw solution; AL-FS, active layer faces feed solution) and applied currents of 0 or 100 mA. (c) Solution conductivities in draw and feed side using a TFC-BW, thin-film composite brackish water, membrane with an AL-DS orientation, with an applied current of 100 mA. The filled arrows indicate when electric current was applied and the empty arrows indicate when current was turned off.

The concentration polarization modulus of the draw (CP_D) and feed (CP_F) for NaCl in the FO compartment were calculated using

$$CP_D = \frac{\pi_{D,m}}{\pi_{D,b}} = \exp\left(-\frac{J_w}{k}\right) \quad (14)$$

$$CP_F = \frac{\pi_{F,m}}{\pi_{F,b}} = \exp\left(\frac{J_w}{k}\right) \quad (15)$$

where $\pi_{D,m}$ is the osmotic pressure at the membrane surface in draw side, $\pi_{D,b}$ is the osmotic pressure of bulk solution in draw side, $\pi_{F,m}$ is the osmotic pressure at the membrane surface in feed side, and $\pi_{F,b}$ is the osmotic pressure of bulk solution in feed side.

The water flux for the symmetric membrane can be calculated as[36]

$$J_w = A\left[\pi_{D,b}\exp\left(-\frac{J_w}{k}\right) - \pi_{F,b}\exp\left(\frac{J_w}{k}\right)\right] \quad (16)$$

Thus, k was calculated by using eq 16 by placing the symmetric membrane in the flow cell. However, since there is significant internal concentration polarization for polyamide-based TFC membranes (TFC-SW and TFC-BW), the term of the solute resistance to diffusion within the porous support layer, K, was used instead of the mass transfer coefficient of the system, k.[37] However, a combination of J_w and k was used to predict CP of salt, as is commonly done in these FO studies.[36] This is because reverse salt flux measured in EFO is different from FO because both sides of the feed chamber is facing to higher saline water stream.[13] In addition, CP in the feed side (CP_F) can be replaced using K as the following equation:

$$K = \frac{t_s\tau}{\varepsilon D} = \frac{S}{D} \quad (17)$$

$$CP_F = \frac{\pi_{F,m}}{\pi_{F,b}} = \exp(J_w K) \quad (18)$$

where t_s is the support layer thickness, τ is the tortuosity, and ε is the porosity of membrane.

The water flux of TFC membranes in FO part was predicted using the following equation:[36]

$$J_w = A\left[\pi_{D,b}\exp\left(-\frac{J_w}{k}\right) - \pi_{F,b}\exp(J_w K)\right] \quad (19)$$

When current was applied in the EFO system, water flux across the membrane was calculated based eq 19 with quantifying osmotic pressure using the van't Hoff equation (see SI note).[38] In the EFO system, there are other ions such as protons and hydroxide ions, but in eq 19, it is assumed that electrical conductivity responds only with sodium and chloride due to the high concentration of both sodium and chloride ions compared to other ions.

The CP modulus for the protons (CP_p) in the draw chamber can be calculated using the following equation:

$$J_w = A\left[\pi_{D,b}\exp\left(-\frac{J_w}{k}\right) - \pi_{F,b}\exp(J_w K) + CP_p(\pi_{D,p} - \pi_{F,p})\right] \quad (20)$$

where $\pi_{D,p}$ is the osmotic pressure of proton of bulk solution in draw side and $\pi_{F,p}$ is the osmotic pressure of proton of bulk solution in feed side. The bulk concentration of protons was calculated from the pH using a pH meter.

RESULTS AND DISCUSSION

Water Flux Enhancement with EFO. Using the TFC-BW membranes in the EFO system, with the active layer facing the draw solution (AL-DS), the water flux increased 5 fold to 5.56 LMH at a set current of 100 mA (1.7 mA cm^{-2}), compared to that obtained in the same system without current (1.10 LMH) (Figure 3a and b). When the membrane orientation was reversed so that the polyamide active layer was facing the feed solution (AL-FS), the flux was 2.13 LMH at a set current of 100 mA (Figure 3b) and 0.71 LMH without current. Since the salt concentration of the draw solution is higher than that of the feed solution in FO, water flux in AL-DS mode is generally higher than AL-FS mode due to the less severe internal concentration polarization of the AL-DS mode.[39] Thus, in the absence of an applied current, the AL-DS mode had slightly higher water flux (1.10 LMH) than the AL-FS mode (0.71 LMH).

The pore size of the active layer of both TFC-BW and TFC-SW membranes is ~0.25 nm.[16,17] However, the permeability (expressed as "water permeability" and "salt permeability" in

DOI: 10.1021/acs.est.9b01481
Environ. Sci. Technol. 2019, 53, 8352−8361

Table 1. Membrane Intrinsic Parameters (A = Water Permeability, B = Salt Permeability, and S = Structural Parameter), Solute Resistance to Diffusion within the Porous Support Layer (K), Concentration Polarization (CP) Modulus of NaCl Ion, and Calculated and Empirical Water Flux with and without Current ($k = 1.34 \times 10^{-4}$ cm/s)[a]

	membrane intrinsic parameters				CP modulus of NaCl		water flux (LMH)	
membrane	A (cm/s- bar)	B (cm/s)	S (cm)	K (s/cm)	draw	feed	I = 0 mA	I = 100 mA
TFC-BW	6.14×10^{-5}	2.46×10^{-6}	0.91 (0.91)	5.68×10^{4} (5.66×10^{4})	0.80	5.70 (5.67)	1.10	1.24 (5.56)
TFC-SW	3.67×10^{-5}	3.80×10^{-7}	3.40 (3.50)	2.11×10^{5} (2.18×10^{5})	0.94	6.53 (6.91)	0.32	N/A

[a]The CP modulus for protons was 1.41×10^{5}. Empirical values are given in parentheses. [b]100 mA (TFC-BW) or 25 mA (TFC-SW) was applied. Water flux of TFC-SW was not calculated because of low applied current (25 mA) due to the high rejection of ions.

Table 1) of the TFC-BW membrane is much greater than TFC-SW membrane because it was developed for brackish water desalination whereas the TFC-SW membrane was designed for seawater desalination. Thus, when the TFC-SW membrane was used in the EFO system, the maximum stable current was 25 mA, due to the high ohmic resistance of this membrane. At a current of 25 mA, the TFC-SW membrane in the AL-DS configuration produced a water flux of 0.70 LMH, which was over twice that obtained without current (0.32 LMH). Water transfer by electro-osmosis (EO), which is defined as a process where charged that move in an electrical field pull along water molecules, was negligible because the water flux enhancement with EFO that was measured here was substantially higher than those reported in the literature (see SI notes).

Current generation in the EFO system resulted in the net production of proton ions at the anode (eq 3), and production of hydroxide ions at the cathode due to hydrogen gas production (eq 4). This production of protons decreased the anolyte effluent pH to 2.7 after ~1000 s of operation, and protons transport through the CEM also decreased the draw solution pH to 2.6 (Figure 3a). The change in pH from pH 7 to pH 2.6 increased in the conductivity of the draw solution by ~0.7 mS cm^{-1} (based on the direct flow of synthetic pH 7 and 2.6 solutions through the conductivity meter). This change in pH would be sufficient to increase conductivity in the draw solution (measured as ~0.8 mS cm^{-1} at 1000 s after operation), and therefore there was likely negligible transport of sodium ions into the draw solution compared to protons. When the current was turned off, the feed solution conductivity increased and returned to its original value due to the flow of fresh feed into the chamber, but the conductivity of the draw solution stayed high likely due to the presence of a greater concentration of protons in the recycling reservoir of the draw solution (Figure 3c). Although both draw and feed solutions were supplied with fresh solutions from each separated reservoirs, a high proton concentration supplied in the draw solution maintained relatively high conductivity.

The release of hydroxide ions from water dissociation and hydrogen production on the cathode increased the catholyte pH to 10.7. As the feed solution became acidic over time, rather than alkaline, the lack of an increase in pH indicated that there was little transport of hydroxide ions through the CEM near the cathode (Figure 3a). Despite continuous migration of protons into the feed chamber, the solution conductivity of the feed decreased when current was applied (Figure 3c). Since the cathode was negatively charged, this decrease in solution conductivity in the feed side was likely due to transport of sodium ions and protons from the feed to the catholyte chamber due to the force maintaining the charge neutrality in each chamber. These changes in pH and conductivity indicated that a current of 100 mA through the TFC-BW membrane was sustained primarily by proton transfer through the two CEMs and the thin-film membrane.

In general, CP is known to have a negative effect on water flux, whether it is concentrative or dilutive.[36] Therefore, this proton accumulation, which positively affects the water flux in the EFO, can be identified as a proton-localized CP to differentiate it from conventional CP based on salt rejection. In the proton-localized CP, the higher the CP, the greater the protons concentration on the draw side of the membrane.

The possibility of water flow across the CEMs in FO without an applied current was examined using an osmotic gradient across the CEMs. No observable water flux across the CEMs was measured with a very stable conductivity change in the feed solution over time, indicating a lack of water flow through the CEMs (SI Figure S2b).

The reverse solute flux was estimated based on changes in conductivity compared to the loss of water (eq 2). With a set current of 100 mA, the conductivity of the feed solution changed by 3.0%, while there was a net water flux change of 1.3% (SI Figure S5, based on the final 10 min of the operation with stabilized conductivities). Thus, the water flux was J_w = 5.56 LMH, and the solute flux was $J_s = 0.37 \times 10^{-5}$ SMH. However, this solute flux is not due to salt from the draw solution as current generation and the pH changes also contributed to the ion flux from the draw solution into the feed solution, and additional ion transport was possible through the CEM facing the catholyte solution. Due to the small changes in the overall salt concentration, a more detailed analysis of the components of the solute flux were not further examined here.

Water Flux in an EFO System in the Absence of Ion Exchange Membranes. An EFO system was examined without two CEMs (and also the associated redox chambers) to demonstrate the importance of the CEMs and proton production for enhancing water flux (Figure 2). In the absence of the two CEMs, the electrodes were placed directly in the feed (cathode) and draw (anode) solutions, with the FO membrane (TFC-BW membrane) facing the draw solution in the middle (Figure 2a). To ensure that the proton concentration in the bulk electrolytes remained relatively constant during the test, 10 mM of HCl was added to electrolytes (initial pH of ~2). In the absence of current, there was a small but net water flux pair into the draw solution of 0.89 LMH. With an applied current of 100 mA, the water flux was highly erratic, with only a net flux of 0.72 LMH by the end of the test (SI Figure S5). This water flux was therefore much lower than that obtained in the EFO process with the two ion exchange membranes (5.56 LMH). The reason for the much lower water flux was likely a consequence of immersion of the anode in the very saline draw solution (257 mM) without the two CEMs, compared to the anolyte solution (145 mM) used with the two CEMs. Current generation by the anode in the more saline NaCl draw solution would have further shifted the

DOI: 10.1021/acs.est.9b01481
Environ. Sci. Technol. 2019, 53, 8352−8361

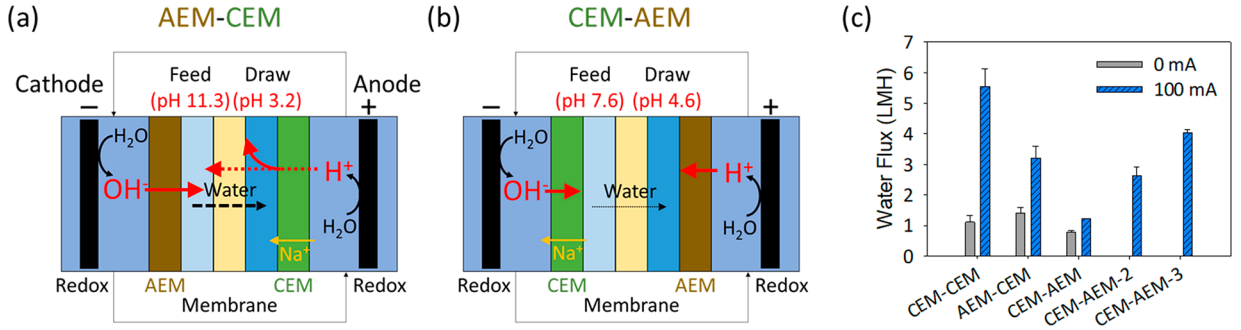

Figure 4. Schematics showing the different combinations of ion exchange membranes used, and the final pHs of the solutions, for pairs of (a) AEM-CEM and (b) CEM-AEM. (c) Water flux depending on the location of ion exchange membranes and operation times: CEM-AEM: 0∼600 s, CEM-AEM-2:900∼1500 s, and CEM-AEM-3:1500∼2000 s). A pair of CEM-CEM was illustrated in Figure 3a. TFC-BW membrane with a AL-DS orientation was used.

dominant reaction from water splitting, which releases protons into solution, to Cl_2 formation due to the higher Cl^- concentration. Formation of Cl_2 from Cl^- ions does not release any protons into solution (eq 6). Thus, moving from a lower to higher Cl^- concentration resulted in a reduction in the generation of protons. From the pH difference before and after operation, there was a greater rate of net proton production at the lower Cl^- concentration in the presence of the two CEMs (0.10 mM min^{-1} of proton) than that obtained with the anode immersed in the draw solution that had a higher concentration of Cl^- (0.08 mM min^{-1} of proton) in the absence of the CEMs. In the absence of the ion exchange membranes, some discoloration of the thin-film membrane was observed following tests with current generation. However, subsequent tests demonstrated that there was insignificant damage to the membrane as there was no appreciable change in water flux (0.87 LMH with no current) in subsequent FO tests (SI Figure S6).

The importance of proton production for enhancing water flux using EFO was further demonstrated by conducting additional tests using nitrate (NO_3^-) instead of Cl^- in the solutions (at pH 2). Nitrate is relatively inert so that changing the nitrate concentration from that of the anolyte (145 mM) to that of the draw solution (257 mM) would not impact proton generation as water splitting would remain the main source of electrons (as opposed to electrons from chloride ion oxidation using NaCl). When the $NaNO_3/HNO_3$ pair was used in EFO system with two CEMs, water flux was significantly increased from 0.63 ± 0.04 (no current) to 3.75 ± 0.13 LMH (100 mA) and the reduction in the feed solution mass was very stable over time (SI Figure S5). When the impact of current was examine in the system without the two CEMs, the water flux without current was very small (0.73 LMH), similar to that obtained with the chloride solution. With current generation and no CEMs, the water flux was again highly erratic, but at the end of the test the net water flux was 3.13 LMH (SI Figure S5), which was similar to that obtained with the two CEMs. The erratic water flux in all cases without the membranes was likely a consequence of gas bubble production which could cause a bending in the thin-film membrane (allowing slight accumulation or losses in chamber volume) and possible disruption of the concentration gradients on the thin-film membrane. Thus, the use of the two redox chambers and two CEMs was required to ensure the stable operation of the system.

Impact of Ion Exchange Membrane Type and Location. To further study the impact of proton transfer on water flux, the CEM membrane near the cathode was replaced with an AEM (AEM-CEM configuration, Figure 4a). The use of the AEM facilitated hydroxide ion transport into the feed solution, increasing its pH to 11.3. The draw solution pH was also slightly higher with this AEM-CEM configuration than the double CEM configuration, likely due to some hydroxide ion transport through the TFC-BW membrane. However, the draw solution pH still remained quite acidic (pH 3.2) due to greater proton transfer from the anolyte chamber into the draw solution (Figure 4a). The use of the AEM reduced the water flux at 100 mA to 3.20 LMH, to slightly more than half that obtained using two CEMs (5.56 LMH) (Figure 4c). Thus, this reduction in water flux was likely due to the greater contribution of hydroxide ion transport that accumulated on the support layer of the membrane decreasing the concentration gradient across the membrane compared to primarily only proton transport using the CEM-CEM membranes.

When the AEM was placed next to the draw solution (CEM-AEM), proton transport into the draw solution was greatly reduced, but not eliminated, as shown by a decrease in the draw solution pH to 4.6 (Figure 4b). In this configuration, the water flux was further decreased to only 1.21 LMH (Figure 4c). The water flux for this CEM-AEM configuration was measured at three different times over the duration of the tests (0−600 s, 900−1500 s, and 1500−2000 s). Because of the small size of protons, an AEM cannot perfectly block the transport of protons.[40,41] Thus, over time, the water flux increased (1.21 LMH, 2.63 LMH, and 4.04 LMH), consistent with the accumulation of protons in the anolyte and through the AEM (Figure 4c). Therefore, these changes in pH support the important role of proton transport enhancing water flow in the EFO system.

Among the three configurations (CEM-CEM, AEM-CEM, and CEM-AEM), the CEM-CEM configuration showed the highest water flux because the process is based on maximizing proton transport from the anode chamber into the draw solution chamber. Therefore, the maximum water flux of the CEM-AEM configuration, with the AEM next to the anode chamber, cannot be higher than that of CEM-CEM configuration as proton transport is hindered by the AEM.

Modeling Concentration Polarization and Water Flux. The impact of proton accumulation on water flux was examined by calculating the membrane intrinsic parameters (A, B, and S), mass transfer coefficient (k), and the solute

DOI: 10.1021/acs.est.9b01481
Environ. Sci. Technol. 2019, 53, 8352−8361

resistance to diffusion within the porous support layer (K). The TFC-BW membrane was more permeable to water and salt than the TFC-SW membrane as shown by higher A and B parameters (Table 1), and a lower structural parameter of the TFC-BW membrane (S = 0.91 cm) than the TFC-SW membrane (S = 3.40 cm). These parameters let to a less resistance to NaCl mass transfer within the TFC-BW membrane (K = 5.68 × 10^4 s cm^{-1}) than the TFC-SW membrane (K = 2.11 × 10^5 s cm^{-1}). The more porous BW membrane therefore had less concentration polarization for NaCl on both the feed and draw sides (CP_D = 0.80, CP_F = 5.70), than those of the SW membrane (CP_D = 0.94, CP_F = 6.53). The higher CP modulus of the feed side reflects the positioning of the active layer of the asymmetric membranes, TFC membranes, facing the draw solution.

A water flux of 1.24 LMH was predicted for the TFC-BW membrane at a set current of 100 mA based on the measured conductivity changes and the calculated CP modulus for NaCl in the feed and draw solutions (Table 1 and eq 19). However, much higher water flux, 5.56 LMH, was observed at a set current of 100 mA. Although it has been reported that electric-current allows the movement of ions in the FO process,[13] it was not as significant as the increase of water flux by a factor of 5 from 1.10 LMH to 5.56 LMH. Thus, it was assumed that increased water flux was mostly attributed to the accumulation of protons that were generated in the EFO system. Based on this discrepancy of the water flux between predicted (1.24 LMH) and observed (5.56 LMH), the CP modulus for protons, CP_D (H^+) = 1.41 × 10^5, was calculated with 100 mA of applied current, and this CP modulus is 5 orders of magnitude higher than the CP modulus for NaCl (CP_D = 0.80), showing the extremely high CP of protons compared to NaCl (Table 1 and eq 20).

Mechanisms of Proton Concentration Polarization. The high CP of protons on the draw side of the membrane was due to the relative size of the hydrated protons (~0.28 nm, versus an ionic radius of ~0.10 nm for hydronium ion) compared to the pore size of a fully cross-linked polyamide layer of a TFC membrane (~0.25 nm).[16,17,42] It has been also reported that protons can hydrate in clusters in the form of $H_9O_4^+$ or $H_5O_2^+$, decreasing their mobilities in aqueous solutions.[43−46] Thus, protons could pass through the pores, but their transport was retarded due to the associated water molecules.

Membrane resistance is also related to the charge of the membrane, which led to a proton rejection of ~44% for the TFC-BW based on measurements in dead-end filtration tests using DI water adjusted to a pH of ~3. The TFC-BW membrane shows a strong positive charge ~pH 3 (surface zeta potential ≈ +20 mV) that can reject proton by electrostatic repulsion.[18,19] Under the same conditions, with 257 mM of NaCl was added into the filtering solution, there was a ~99% rejection of protons. This is because hydrated chloride ion, larger in size than the pores of the TFC-BW membrane, do not easily pass through the membrane, but attract the positive proton by the electrical attraction (SI Figure S7). Due to this Donnan effect,[47] the proton removal rate of the TFC-BW membrane was drastically increased to ~99% by adding NaCl. It has been also reported that cation transport across a TFC membrane in FO varies significantly with pH change and occurred slowest at acidic pH.[48]

Proton migration was further examined using the EFO cell as osmotic pressure and hydraulic pressure are not identical driving forces.[49] When the initial solution pHs were set at 3 for the feed side and 11 for the draw side (SI Figure S8), the resulting changes in solution conductivities in the feed solution showed a similar trend over time to that obtained when the initial pH was near neutral for the TFC-BW membrane, indicating the TFC-BW membrane rejected most of the protons when operated without an applied current. However, as indicated from pH changes in both draw and feed solutions (Figures 3a and 4a,b), protons can pass through the TFC-BW membrane to sustain current when a set current of 100 mA was applied in the EFO system.

The Role of Initial Proton Concentration and Current. The impact of the solution pH was examined by changing the pH of the chambers to those obtained at the end of a test, and comparing the water flux with and without current generation. Therefore, the initial pH conditions were set as follows: redox chambers (pH-R), pH 3 (the anode chamber) or 11 (the cathode chamber); draw chamber, pH 3, and feed chamber, pH 11 (Figure 5a). Without current, the same water fluxes were measured in all cases, demonstrating a lack of an impact of the starting pH. When a current (100 mA) was applied, the water flux increased to the same amount also for all cases. Therefore, the current and not the initial concentration of protons was primarily responsible for the improved water flux for the EFO system. Water flux was also demonstrated to be proportional to the applied current, by setting it at 10, 50, and 100 mA, compared to a control (no current) (Figure 5b). This implies that the electric current plays an important role in bringing protons closer to the membrane surface to provide a

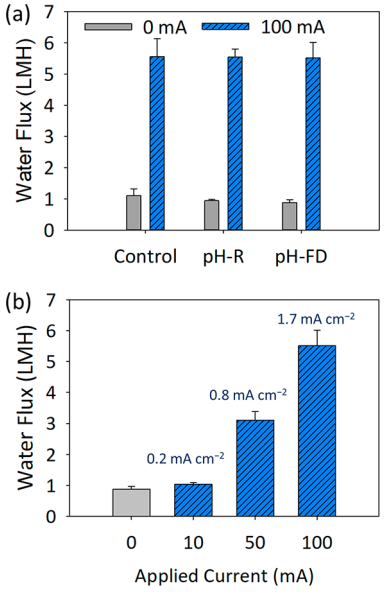

Figure 5. (a) Water flux as a function of pH and applied current: no pH adjustment (control), initial pHs were adjusted in redox (pH-R) or feed/draw solutions (pH-FD). Solutions pH near the anode (draw and redox chamber in the anode) were adjusted as pH 3 using HCl and those near the cathode (feed and redox chamber in the cathode) were controlled as pH 11 using NaOH to make the similar environment as operating solutions. (b) The relationship between water flux and applied current from 0−100 mA in case of initial pHs of feed (pH 11) and draw (pH 3) solutions were adjusted. Applied current density (mA cm^{-2}) is described on each applied current (bar). The TFC-BW membrane with a AL-DS orientation was used.

DOI: 10.1021/acs.est.9b01481
Environ. Sci. Technol. 2019, 53, 8352−8361

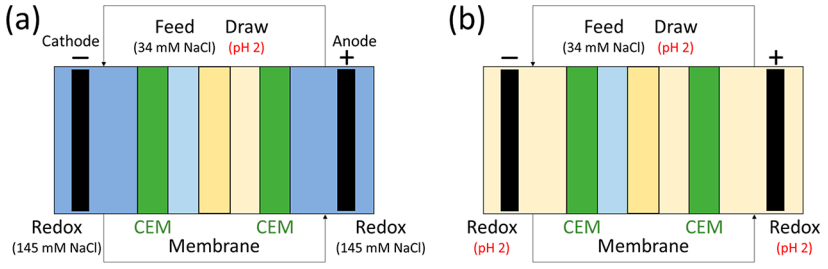

Figure 6. Schematics of the EFO system using pH 2 solution as (a) draw solution or (b) draw and redox solutions without adding any NaCl. Solution pHs were adjusted using HCl to be 10 mM.

greater osmotic pressure due to the high localized concentration of protons.

Water Flux in the Absence of a High Salt Draw Solution. To determine the impact the current separate from that of the draw solution, the concentration of the draw solution was reduced from 247 mM to 10 mM. Even without a high concentration draw solution, the water flux was 2.24 ± 0.31 LMH at a current of 100 mA (Figure 6a). In the absence of the current, a reverse water flux of −0.17 ± 0.05 LMH was measured (water flow from the draw to feed solution) due to the higher salt concentration of the feed solution (34 mM NaCl) compared to that in the draw solution chamber (10 mM HCl). When both the anolyte and catholyte chambers were also filled with 10 mM HCl (instead of 145 mM NaCl), the water flux was 1.39 ± 0.07 LMH at an applied current of 100 mA (Figure 6b). In contrast, a reverse water flux of −0.40 ± 0.00 LMH was obtained without any current. As a result, in the EFO system, when an electric current is applied, most of the protons migrated from the anode to the draw accumulate on the membrane surface, improving the osmotic pressure across the membrane. Therefore, the current enabled to increase water flux across the membrane regardless of the concentration of draw solute and even the presence of the negative driving force.

Outlook. The EFO system provides a new approach for increasing water flux across an FO membrane. This system could be used for FO applications where a high osmotic pressure is required with limited use of draw solute, such as desalination, beverage concentrate production, and fertilizer dilution, as the osmotic pressure can be better controlled through current generation.

To render the EFO system more practical in wider applications, there are several issues need to be addressed. First, since the current EFO system operates based on water electrolysis, its energy demand is high (~8.84 kWh m^{-3} at 100 mA and 2.9 V). In order to lower this, it would be necessary to lower the operating voltage by using electrodes with lower overpotentials, and developing more optimal membranes for the EFO process. However, this process, similar to the "shock electrodialysis",[7,8] is currently dependent on water splitting. It might be possible to further reduce the voltage needed at the anode, for example by using bioanodes[50] or more thermodynamically favorable reactions at the anode, as long as they produce protons in proportion to the electrical current. Other operating conditions, such as different concentrations (feed/draw/redox solutions) and flow rates as well as membrane stability at the wide range of pH (from 2.6 to 10.7) should be also examined to further improve performance or reduce energy consumption. According to the manufacturer, the TFC-BW membrane can be continuously operated over a pH range of 2−11. However, the manufacturer recommends the narrow pH range (pH 5−7) for IEMs for long-term operation. The use of the EFO process would benefit from the use of membranes that are more resistant to high and low pHs, and additional research on neutralizing solutions pHs after operation since discharging very low pH solutions needs to be avoided in terms of environmental impact. In addition, different types of membranes including TFC and cellulose-based membranes that are used in FO should be further tested. Since membrane fouling occurs at the membrane surface where the membrane contacts the feed solution, long-term operation of the EFO process using different membrane orientations should be further examined to minimize membrane fouling as the AL-DS orientation is more prone to fouling than the AL-FS orientation.[51]

■ ASSOCIATED CONTENT

Supporting Information

The Supporting Information is available free of charge on the ACS Publications website at DOI: 10.1021/acs.est.9b01481.

Details on the Sherwood correlation, mass transfer coefficient, van't Hoff equation, the effect of electro-osmosis and ion depletion zone by current, and the measurement of reverse solute flux (Text). The comparison of water flux enhancement depending on redox compound (Table S1), the photographs of the EFO cell (Figure S1), the EFO at the null-osmosis (Figure S2), the schematic and voltage profiles of the EFO using potassium ferri/ferrocyanide redox couples (Figure S3), the reverse solute flux depending on the different orientation of the membrane or different location of ion exchange membrane (Figure S4), the changes of the feed solution mass with and without CEMs (Figure S5), the photographs of the membranes before and after applying current (Figure S6), the schematic illustration of proton rejection by the TFC-BW membrane (Figure S7), and the conductivity profile of the feed solution effluent over time (Figure S8) (PDF)

■ AUTHOR INFORMATION

Corresponding Author

*Phone: +1-814-863-7908; e-mail: blogan@psu.edu.

ORCID

Moon Son: 0000-0002-3770-148X
Taeyoung Kim: 0000-0003-0346-5519
Wulin Yang: 0000-0003-3590-5080
Christopher A. Gorski: 0000-0002-5363-2904
Bruce E. Logan: 0000-0001-7478-8070

DOI: 10.1021/acs.est.9b01481
Environ. Sci. Technol. 2019, 53, 8352−8361

Notes

The authors declare no competing financial interest.

■ ACKNOWLEDGMENTS

We thank Dr. Manish Kumar and Mr. Woochul Song at Pennsylvania State University for the loan of the dead-end filtration test device. This research was supported by the King Abdullah University of Science and Technology (KAUST) (OSR-2017-CPF-2907-02) and Pennsylvania State University.

■ REFERENCES

(1) Cath, T. Y.; Childress, A. E.; Elimelech, M. Forward osmosis: Principles, applications, and recent developments. *J. Membr. Sci.* **2006**, *281* (1), 70−87.

(2) Liu, Z.; Bai, H.; Lee, J.; Sun, D. D. A low-energy forward osmosis process to produce drinking water. *Energy Environ. Sci.* **2011**, *4* (7), 2582−2585.

(3) Blandin, G.; Verliefde, A. R. D.; Tang, C. Y.; Childress, A. E.; Le-Clech, P. Validation of assisted forward osmosis (AFO) process: Impact of hydraulic pressure. *J. Membr. Sci.* **2013**, *447* (15), 1−11.

(4) Sahebi, S.; Phuntsho, S.; Kim, J. E.; Hong, S.; Shon, H. K. Pressure assisted fertiliser drawn osmosis process to enhance final dilution of the fertiliser draw solution beyond osmotic equilibrium. *J. Membr. Sci.* **2015**, *481* (1), 63−72.

(5) Duan, J.; Litwiller, E.; Pinnau, I. Solution-diffusion with defects model for pressure-assisted forward osmosis. *J. Membr. Sci.* **2014**, *470* (15), 323−333.

(6) Oh, Y.; Lee, S.; Elimelech, M.; Lee, S.; Hong, S. Effect of hydraulic pressure and membrane orientation on water flux and reverse solute flux in pressure assisted osmosis. *J. Membr. Sci.* **2014**, *465* (1), 159−166.

(7) Deng, D.; Dydek, E. V.; Han, J.-H.; Schlumpberger, S.; Mani, A.; Zaltzman, B.; Bazant, M. Z. Overlimiting current and shock electrodialysis in porous media. *Langmuir* **2013**, *29* (52), 16167−16177.

(8) Schlumpberger, S.; Lu, N. B.; Suss, M. E.; Bazant, M. Z. Scalable and continuous water deionization by shock electrodialysis. *Environ. Sci. Technol. Lett.* **2015**, *2* (12), 367−372.

(9) Zhang, S.; Wang, K. Y.; Chung, T.-S.; Chen, H.; Jean, Y. C.; Amy, G. Well-constructed cellulose acetate membranes for forward osmosis: Minimized internal concentration polarization with an ultra-thin selective layer. *J. Membr. Sci.* **2010**, *360* (1), 522−535.

(10) Wang, K. Y.; Ong, R. C.; Chung, T.-S. Double-skinned forward osmosis membranes for reducing internal concentration polarization within the porous sublayer. *Ind. Eng. Chem. Res.* **2010**, *49* (10), 4824−4831.

(11) Li, M.; Karanikola, V.; Zhang, X.; Wang, L.; Elimelech, M. A self-standing, support-free membrane for forward osmosis with no internal concentration polarization. *Environ. Sci. Technol. Lett.* **2018**, *5* (5), 266−271.

(12) Zhou, S.; Liu, F.; Wang, J.; Lin, H.; Han, Q.; Zhao, S.; Tang, C. Y. Janus membrane with unparalleled forward osmosis performance. *Environ. Sci. Technol. Lett.* **2019**, *6* (2), 79−85.

(13) Zou, S.; He, Z. Electrolysis-assisted mitigation of reverse solute flux in a three-chamber forward osmosis system. *Water Res.* **2017**, *115* (15), 111−119.

(14) Liu, Q.; Qiu, G.; Zhou, Z.; Li, J.; Amy, G. L.; Xie, J.; Lee, J. Y. An Effective Design of Electrically Conducting Thin-Film Composite (TFC) Membranes for Bio and Organic Fouling Control in Forward Osmosis (FO). *Environ. Sci. Technol.* **2016**, *50* (19), 10596−10605.

(15) Zhou, K. G.; Vasu, K. S.; Cherian, C. T.; Neek-Amal, M.; Zhang, J. C.; Ghorbanfekr-Kalashami, H.; Huang, K.; Marshall, O. P.; Kravets, V. G.; Abraham, J.; Su, Y.; Grigorenko, A. N.; Pratt, A.; Geim, A. K.; Peeters, F. M.; Novoselov, K. S.; Nair, R. R. Electrically controlled water permeation through graphene oxide membranes. *Nature* **2018**, *559* (7713), 236−240.

(16) Kim, S.-J.; Han, D.; Yu, H.-W.; O'Rourke, B. E.; Kobayashi, Y.; Suzuki, R.; Hwang, M.; Kim, I. S. Performance evaluation of polyamide TFC membranes: Effects of free volume properties on boron transport. *Desalination* **2018**, *432* (15), 104−114.

(17) Kim, S.-J.; Kook, S.; O'Rourke, B. E.; Lee, J.; Hwang, M.; Kobayashi, Y.; Suzuki, R.; Kim, I. S. Characterization of pore size distribution (PSD) in cellulose triacetate (CTA) and polyamide (PA) thin active layers by positron annihilation lifetime spectroscopy (PALS) and fractional rejection (FR) method. *J. Membr. Sci.* **2017**, *527* (1), 143−151.

(18) Idil Mouhoumed, E.; Szymczyk, A.; Schäfer, A.; Paugam, L.; La, Y. H. Physico-chemical characterization of polyamide NF/RO membranes: Insight from streaming current measurements. *J. Membr. Sci.* **2014**, *461* (1), 130−138.

(19) Kezia, K.; Lee, J.; Hill, A. J.; Kentish, S. E. Convective transport of boron through a brackish water reverse osmosis membrane. *J. Membr. Sci.* **2013**, *445* (15), 160−169.

(20) Geise, G. M.; Cassady, H. J.; Paul, D. R.; Logan, B. E.; Hickner, M. A. Specific ion effects on membrane potential and the permselectivity of ion exchange membranes. *Phys. Chem. Chem. Phys.* **2014**, *16* (39), 21673−21681.

(21) Le, X. T.; Bui, T. H.; Viel, P.; Berthelot, T.; Palacin, S. On the structure−properties relationship of the AMV anion exchange membrane. *J. Membr. Sci.* **2009**, *340* (1), 133−140.

(22) Kim, T.; Logan, B. E.; Gorski, C. A. High power densities created from salinity differences by combining electrode and Donnan potentials in a concentration flow cell. *Energy Environ. Sci.* **2017**, *10* (4), 1003−1012.

(23) Pan, S.-Y.; Snyder, S. W.; Lin, Y. J.; Chiang, P.-C. Electrokinetic desalination of brackish water and associated challenges in the water and energy nexus. *Environ. Sci.: Water Res. Technol.* **2018**, *4* (5), 613−638.

(24) Shukla, A. K.; Ravikumar, M. K.; Balasubramanian, T. S. Nickel/iron batteries. *J. Power Sources* **1994**, *51* (1), 29−36.

(25) Rajkumar, D.; Kim, J. G. Oxidation of various reactive dyes with in situ electro-generated active chlorine for textile dyeing industry wastewater treatment. *J. Hazard. Mater.* **2006**, *136* (2), 203−212.

(26) Ichihashi, K.; Teranishi, K.; Ichimura, A. Brominated trihalomethane formation in halogenation of humic acid in the coexistence of hypochlorite and hypobromite ions. *Water Res.* **1999**, *33* (2), 477−483.

(27) Mostafa, E.; Reinsberg, P.; Garcia-Segura, S.; Baltruschat, H. Chlorine species evolution during electrochlorination on boron-doped diamond anodes: In-situ electrogeneration of Cl_2, Cl_2O and ClO_2. *Electrochim. Acta* **2018**, *281* (10), 831−840.

(28) Pillai, K. C.; Kwon, T. O.; Park, B. B.; Moon, I. S. Studies on process parameters for chlorine dioxide production using IrO_2 anode in an un-divided electrochemical cell. *J. Hazard. Mater.* **2009**, *164* (2), 812−819.

(29) Wang, T. X.; Margerum, D. W. Kinetics of reversible chlorine hydrolysis: temperature dependence and general-acid/base-assisted mechanisms. *Inorg. Chem.* **1994**, *33* (6), 1050−1055.

(30) Son, M.; Park, H.; Liu, L.; Choi, H.; Kim, J. H.; Choi, H. Thin-film nanocomposite membrane with CNT positioning in support layer for energy harvesting from saline water. *Chem. Eng. J.* **2016**, *284* (15), 68−77.

(31) Son, M.; Choi, H.-g.; Liu, L.; Celik, E.; Park, H.; Choi, H. Efficacy of carbon nanotube positioning in the polyethersulfone support layer on the performance of thin-film composite membrane for desalination. *Chem. Eng. J.* **2015**, *266* (15), 376−384.

(32) Yip, N. Y.; Tiraferri, A.; Phillip, W. A.; Schiffman, J. D.; Elimelech, M. High performance thin-film composite forward osmosis membrane. *Environ. Sci. Technol.* **2010**, *44* (10), 3812−3818.

(33) Vrouwenvelder, J. S.; van Paassen, J. A. M.; van Agtmaal, J. M. C.; van Loosdrecht, M. C. M.; Kruithof, J. C. A critical flux to avoid biofouling of spiral wound nanofiltration and reverse osmosis membranes: Fact or fiction? *J. Membr. Sci.* **2009**, *326* (1), 36−44.

(34) Tang, C. Y.; She, Q.; Lay, W. C. L.; Wang, R.; Fane, A. G. Coupled effects of internal concentration polarization and fouling on

DOI: 10.1021/acs.est.9b01481
Environ. Sci. Technol. 2019, 53, 8352−8361

flux behavior of forward osmosis membranes during humic acid filtration. *J. Membr. Sci.* **2010**, *354* (1), 123−133.
(35) Park, M.; Lee, J. J.; Lee, S.; Kim, J. H. Determination of a constant membrane structure parameter in forward osmosis processes. *J. Membr. Sci.* **2011**, *375* (1), 241−248.
(36) McCutcheon, J. R.; Elimelech, M. Influence of concentrative and dilutive internal concentration polarization on flux behavior in forward osmosis. *J. Membr. Sci.* **2006**, *284* (1), 237−247.
(37) Tiraferri, A.; Yip, N. Y.; Phillip, W. A.; Schiffman, J. D.; Elimelech, M. Relating performance of thin-film composite forward osmosis membranes to support layer formation and structure. *J. Membr. Sci.* **2011**, *367* (1), 340−352.
(38) Zhou, Z.; Lee, J. Y.; Chung, T.-S. Thin film composite forward-osmosis membranes with enhanced internal osmotic pressure for internal concentration polarization reduction. *Chem. Eng. J.* **2014**, *249* (1), 236−245.
(39) Ma, N.; Wei, J.; Qi, S.; Zhao, Y.; Gao, Y.; Tang, C. Y. Nanocomposite substrates for controlling internal concentration polarization in forward osmosis membranes. *J. Membr. Sci.* **2013**, *441*, 54−62.
(40) Zhu, X.; Logan, B. E. Microbial electrolysis desalination and chemical-production cell for CO_2 sequestration. *Bioresour. Technol.* **2014**, *159*, 24−29.
(41) Grib, H.; Bonnal, L.; Sandeaux, J.; Sandeaux, R.; Gavach, C.; Mameri, N. Extraction of amphoteric amino acids by an electro-membrane process. pH and electrical state control by electrodialysis with bipolar membranes. *J. Chem. Technol. Biotechnol.* **1998**, *73* (1), 64−70.
(42) Nightingale, E., Jr Phenomenological theory of ion solvation. Effective radii of hydrated ions. *J. Phys. Chem.* **1959**, *63* (9), 1381−1387.
(43) Wicke, E.; Eigen, M.; Ackermann, T. über den Zustand des Protons (Hydroniumions) in wässriger Lösung. *Z. Phys. Chem.* **1954**, *1*, 340−364.
(44) Eigen, M. Proton transfer, acid-base catalysis, and enzymatic hydrolysis. *Angew. Chem., Int. Ed. Engl.* **1964**, *3* (1), 1−19.
(45) Headrick, J. M.; Diken, E. G.; Walters, R. S.; Hammer, N. I.; Christie, R. A.; Cui, J.; Myshakin, E. M.; Duncan, M. A.; Johnson, M. A.; Jordan, K. D. Spectral signatures of hydrated proton vibrations in water clusters. *Science* **2005**, *308* (5729), 1765−1769.
(46) Marx, D.; Tuckerman, M. E.; Hutter, J.; Parrinello, M. The nature of the hydrated excess proton in water. *Nature* **1999**, *397* (6720), 601.
(47) Levenstein, R.; Hasson, D.; Semiat, R. Utilization of the Donnan effect for improving electrolyte separation with nanofiltration membranes. *J. Membr. Sci.* **1996**, *116* (1), 77−92.
(48) Arena, J. T.; Chwatko, M.; Robillard, H. A.; McCutcheon, J. R. pH sensitivity of ion exchange through a thin film composite membrane in forward osmosis. *Environ. Sci. Technol. Lett.* **2015**, *2* (7), 177−182.
(49) Kook, S.; Swetha, C. D.; Lee, J.; Lee, C.; Fane, T.; Kim, I. S. Forward osmosis membranes under null-pressure condition: Do hydraulic and osmotic pressures have identical nature? *Environ. Sci. Technol.* **2018**, *52* (6), 3556−3566.
(50) Lu, L.; Vakki, W.; Aguiar, J. A.; Xiao, C.; Hurst, K.; Fairchild, M.; Chen, X.; Yang, F.; Gu, J.; Ren, Z. J. Unbiased solar H2 production with current density up to 23 mA cm−2 by Swiss-cheese black Si coupled with wastewater bioanode. *Energy Environ. Sci.* **2019**, *12* (3), 1088−1099.
(51) Mi, B.; Elimelech, M. Chemical and physical aspects of organic fouling of forward osmosis membranes. *J. Membr. Sci.* **2008**, *320* (1−2), 292−302.

DOI: 10.1021/acs.est.9b01481
Environ. Sci. Technol. 2019, 53, 8352−8361